N 62 70451

NASA TR R-27

NASA TR R-27

NATIONAL AERONAUTICS AND SPACE ADMINISTRATION

IN-77

380351

TECHNICAL REPORT
R-27

THEORETICAL AND EXPERIMENTAL INVESTIGATION OF HEAT CONDUCTION IN AIR, INCLUDING EFFECTS OF OXYGEN DISSOCIATION

By C. FREDERICK HANSEN, RICHARD A. EARLY,
FREDERICK E. ALZOFON, and FRED C. WITTEBORN

1959

For sale by the Superintendent of Documents, U.S. Government Printing Office, Washington 25, D.C. Yearly subscription, $10; foreign, $13;
single copy price varies according to size - - - - - - - - - Price 40 cents

TECHNICAL REPORT R-27

THEORETICAL AND EXPERIMENTAL INVESTIGATION OF HEAT CONDUCTION IN AIR, INCLUDING EFFECTS OF OXYGEN DISSOCIATION

By C. FREDERICK HANSEN, RICHARD A. EARLY,
FREDERICK E. ALZOFON, and FRED C. WITTEBORN

Ames Research Center
Moffett Field, Calif.

TECHNICAL REPORT R-27

THEORETICAL AND EXPERIMENTAL INVESTIGATION OF HEAT CONDUCTION IN AIR, INCLUDING EFFECTS OF OXYGEN DISSOCIATION

By C. Frederick Hansen, Richard A. Early, Frederick E. Alzofon, and Fred C. Witteborn

SUMMARY

The one-dimensional, nonsteady flow of heat through gases at constant pressure is considered where the coefficients of thermal conductivity and diffusivity are functions of temperature. For ideal gases, the diffusivity is taken to be directly proportional to the integral of thermal conductivity. In the case of air, it is further assumed that the diffusivity becomes a constant in the temperature interval where oxygen dissociation occurs. These assumptions facilitate numerical solution of the heat flow equation for the case of a semi-infinite gas medium with a constant initial temperature and a constant boundary temperature. The solutions are used, along with measured shock velocity and the measured heat flux through a surface from which the shock wave reflects, in order to evaluate the integral of thermal conductivity as a function of temperature. This integral replaces temperature as the dependent variable for heat conduction in media which have a variable coefficient of thermal conductivity. The experimental results agree with theoretical estimates within the accuracy of the measurements and within the uncertainty in theory.

INTRODUCTION

In the classical solutions for heat transfer by conduction, it has usually been assumed that the coefficients of thermal conductivity and of diffusivity are constant (see refs. 1 and 2, for example). This assumption is quite good for many solids and liquids if the absolute temperature throughout the medium does not vary by large factors. In gases, on the other hand, the coefficient of thermal conductivity is approximately proportional to the half power of temperature if the gas is inert (ref. 3). For constant pressure processes, the diffusivity of an inert gas is approximately proportional to the three-halves power of temperature. Even greater variations with temperature occur in gases which are chemically reactive. Thus, the classical heat-conduction solutions apply to gases only where the differences in absolute temperature throughout the gas are very small. This condition is not fulfilled in many practical heat-conduction problems, of course. For example, it has been shown that, neglecting radiation, the heat transfer occurs essentially by a conduction process at the stagnation region of vehicles traveling at high speed through the atmosphere (ref. 4). Within this same region, the temperature, and therefore the other properties of the gas, changes by large factors. This heat-conduction problem is further complicated by the fact that the air molecules may dissociate in the flow around vehicles flying faster than about 7,000 feet per second. In addition, appreciable ionization may occur at speeds above 30,000 feet per second. Such chemical reactions absorb heat in regions where dissociation and ionization occur and liberate heat again in regions of recombination, thus behaving like heat sinks and heat sources in the gas, respectively. Nernst (ref. 5) shows that such effects can strongly influence the heat-conduction characteristics of the gas.

The steady-state heat-conduction problem can be characterized in terms of the temperature and the coefficient of thermal conductivity, provided reaction rates are rapid enough to insure chemical equilibrium locally throughout the gas. Hirschfelder (ref. 6) has analyzed the one-dimensional, steady-state heat conduction in a chemically reacting gas in which large variations in the coefficient of thermal conductivity appear. Coffin and O'Neal have experimentally verified Hirschfelder's results for the case of dissociating N_2O_4 (ref. 7). In the case of nonsteady heat conduction the coefficient of thermal diffusivity also appears. It is the purpose of this paper to develop solutions for one-dimensional, nonsteady heat conduction in gases at constant pressure that take into account variations in both the coefficients of thermal conductivity and diffusivity. These solutions will be used in conjunction with experimental measurements in a shock tube for the purpose of evaluating an average coefficient of thermal conductivity as a function of temperature.

SYMBOLS

a	coefficient of thermal diffusivity, $\frac{k}{\rho C_p}$
b_i	stoichiometric coefficient for component B_i in a chemical reaction (eq. (21))
B_i	reacting chemical component
C	specific heat per unit mass
D_{ij}	binary mass diffusion coefficient for diffusion of particles type i into particles type j
k	coefficient of thermal conductivity
$\bar{k}$	coefficient k averaged over temperature, $\frac{1}{T}\int_0^T k\,dT$
K_p	chemical equilibrium constant in terms of partial pressures
n	exponent of temperature giving the variation of k with temperature, also the number of mols of gas per unit volume
p	pressure
q	heat flux per unit area
R	gas constant per unit mass
t	time
T	absolute temperature of gas medium
T_c	temperature at which the coefficient of thermal conductivity is a maximum
T_o	temperature at the interface between gas and solid media, also used as a standard reference condition
T_s	initial temperature of solid medium
w	dimensionless variable, $y\sqrt{\frac{a_0}{a_\infty}}$
x	distance
x_i	mol fraction of the ith component of a gas mixture
y	dimensionless variable, $\frac{x}{\sqrt{4a_0t}}$
z	dimensionless integral of thermal conductivity, $\frac{\varphi}{\varphi_0}$
z^*	reference value for the parameter z (see eq. (16))
$z_\infty{}^*$	reference for the limiting value of z (see eq. (19))
α	coefficient of resistance change with temperature
ρ	density
φ	integral of thermal conductivity, $\int_0^T k\,dT$
φ^*	value of the parameter φ for normal air, $\frac{2}{3}k_0T_0\left(\frac{T}{T_0}\right)^{3/2}$
∇	gradient operator
erf y	$\frac{2}{\sqrt{\pi}}\int_0^y e^{-u^2}du$

SUBSCRIPTS

0	conditions at temperature T_0, also the condition at the interface between gas and solid media
1	initial conditions in the shock tube
2	conditions following the initial shock wave produced in the shock tube
3	conditions following the reflection of the initial shock wave
4	initial conditions in the shock-tube reservoir
∞	initial conditions in the gas medium, identified with condition 3 in the shock-tube experiments
c	conditions at temperature T_c
p	conditions in the gas state at constant pressure
s	conditions in the solid state medium bounding the gas phase

THEORETICAL CONSIDERATIONS

The problem which will be considered is the nonsteady, one-dimensional heat conduction through a semi-infinite gas medium at constant pressure with uniform initial conditions. First, the analysis will treat the conduction of heat through an ideal gas to a constant temperature reservoir. Next, the same problem will be considered for a gas which is chemically reactive, such as dissociating air. Finally, the analysis will treat the heat conduction through the gas to a semi-infinite solid which also has uniform initial conditions.

The partial differential equation which describes nonsteady heat flow by conduction is the familiar diffusion equation

$$C_p\rho\frac{\partial T}{\partial t}-\nabla(k\nabla T)=0 \tag{1}$$

The temperature T is the dependent variable, C_p is the specific heat per unit mass, and ρ is the density of the medium. Usually, the coefficient of thermal conductivity k is considered constant so that it can be taken outside the differential operator. However, for the problem of interest here, conduction of heat through gases, k must be treated as a variable. In such problems it is generally permissible to treat the coefficient k as a function of temperature only, however. Then a useful transformation is

$$\varphi=\int_0^T kdT\equiv\bar{k}T \tag{2}$$

and the differential equation (1) can be put into the form

$$\frac{\partial\varphi}{\partial t}-a\nabla^2\varphi=0 \tag{3}$$

where a is the thermal diffusivity

$$a=\frac{k}{C_p\rho} \tag{4}$$

It may be noted that equation (2) is the same as the Kirchoff transformation referred to by Jakob (ref. 2), and has also been used by Langmuir (ref. 8) in calculating the rate of heat loss from solid surfaces immersed in a gas. Crank (ref. 9) uses a similar transformation in treating some mass diffusion problems.

It is apparent from equation (3) that all of the heat-conduction solutions which have been worked out on the basis of a constant thermal conductivity apply equally well to media for which thermal conductivity varies with temperature if the thermal diffusivity is relatively constant. The function φ merely takes the place of temperature as the dependent variable in these solutions. This function is the product of the temperature and an average coefficient of thermal conductivity (eq. (2)). It may be noted that the lower limit of the averaging integral is arbitrary, just as the reference level normally used for temperature is arbitrary. Absolute zero is used as the lower limit here as a convenience. The heat flux at any position is just the gradient of the φ function at that point in the medium.

$$q=-\text{grad }\varphi \tag{5}$$

HEAT CONDUCTION THROUGH AN IDEAL GAS

In the case of gases, the differential equation (3) must be solved with a variable coefficient of diffusivity. For ideal gases the approximation is made that k varies as the nth power of temperature and that the density ρ is given by the ideal gas law. Then the diffusivity is

$$a=\frac{Rk_0}{pC_pT_0^n}T^{n+1} \tag{6}$$

and the φ function is

$$\varphi=\frac{k_0}{(n+1)T_0^n}T^{n+1} \tag{7}$$

where the subscript zero refers to values at some standard condition. Thus, diffusivity is proportional to φ

$$a=\frac{(n+1)R}{pC_p}\varphi \tag{8}$$

This relation is reliable over a considerable range of temperature for monatomic gases and is a reasonably good approximation for many polyatomic gases, including common diatomic gases, such as hydrogen, oxygen, and nitrogen. Sometimes a better approximation is given by a linear relation with a finite intercept, but this can always be transformed to a direct proportionality by appropriate adjustment of the lower limit for the integral φ. In the integrations which follow, it will be necessary to use only the result that the diffusivity a is approximately proportional to φ.

Consider now the nonsteady, one-dimensional flow of heat into a constant temperature reservoir from a semi-infinite medium. The heat-conduction equation reduces to

$$\frac{\partial\varphi}{\partial t}-a\frac{\partial^2\varphi}{\partial x^2}=0 \tag{9}$$

Boltzmann (see ref. 9 or 10) has shown that for certain boundary conditions, and provided that the coefficient of diffusivity is a function of the dependent variable only, the solution to equation (9) may be expressed as a function of $x/\sqrt{t}$. This occurs when the boundary conditions in both time and space can also be expressed as functions of $x/\sqrt{t}$ alone, so that x and t are not involved separately. In the present case, the diffusivity is taken to be a function of φ alone, and the boundary conditions are constant, independent of x and t. Therefore the solution may be given as a function of the dimensionless time-distance parameter

$$y=\frac{x}{\sqrt{4a_0t}} \tag{10}$$

It will also be convenient to make the dependent variable dimensionless with the transformation

$$z=\varphi/\varphi_0 \tag{11}$$

Then the partial differential equation (9) becomes the ordinary differential equation

$$\frac{a}{a_0}\frac{d^2z}{dy^2}+2y\frac{dz}{dy}=0 \tag{12}$$

The factor 4 under the radical of equation (10) is an arbitrary stretching factor chosen so that the dependent variable reduces to its usual form in the case where diffusivity is constant. The standard state will be taken as the constant conditions which exist at the boundary between the conducting medium and the reservoir at $x=0$. Then the boundary conditions are

$$z_0=1 \tag{13a}$$

$$z_\infty=\varphi_\infty/\varphi_0 \tag{13b}$$

Where a is proportional to φ, equation (12) becomes

$$z\frac{d^2z}{dy^2}+2y\frac{dz}{dy}=0 \tag{14}$$

It does not seem promising to seek an exact analytic solution to equation (14) which will satisfy the given initial and boundary conditions. However, if one specifies the value of $(dz/dy)_0$, it becomes relatively easy to integrate the equation numerically. Some results of integrations of equation (14) are shown in figure 1 and table I.

For convenience in plotting, the variable y is replaced by w

$$w=\sqrt{\frac{a_0}{a_\infty}}\,y \tag{15}$$

so that z will approach its limit in each case at about the same point, that is where w is approximately 2.0. It is also convenient to use the function.

$$z^*=1+(z_\infty-1)\ \mathrm{erf}\ w \tag{16}$$

as a normalizing parameter so that the solutions can be plotted accurately on a single graph for a wide range of conditions. The parameter z^* is

TABLE I.—BOUNDARY CONDITIONS IN A SEMI-INFINITE GAS MEDIUM WITH A CONSTANT INITIAL TEMPERATURE, T_∞, AND A CONSTANT BOUNDARY TEMPERATURE, T_0

$$z=\frac{\int_0^T k\,dT}{\int_0^{T_0} k\,dT}$$

$$y=\frac{x}{\sqrt{4a_0t}}$$

z_0	$\left(\frac{dz}{dy}\right)_0$	z_∞
1.0	0.2	1.187
	.4	1.395
	.6	1.625
	.8	1.876
	1.0	2.149
	1.2	2.446
	1.4	2.765
	1.6	3.108
	1.8	3.475
	2.0	3.866
	2.2	4.281
	2.4	4.722
	2.6	5.187
	2.8	5.677
	3.0	6.193
	4.0	9.158
	5.0	12.780
	6.0	17.070
	7.0	22.038
	8.0	27.691
	9.0	34.033
	10.0	41.069
	11.0	48.801
	12.0	57.232
	13.0	66.365
	14.0	76.200
	15.0	86.739
	20.0	150.029
	25.0	231.040
	30.0	329.821

just the function to which z reduces in the case where thermal diffusivity is constant.

Figure 1(a) shows the ratio z/z^* for specific values of the limit z_∞, which have been obtained by numerical integration of equation (14). The initial slopes corresponding to these values of z_∞ may be found in table I. The ratio z/z^* is everywhere larger than unity and goes through a distinct maximum. The effect is more pronounced the larger the value of z_∞. The integral φ, however, is a smooth, monotonically increasing function of w or y, similar to the error function in appearance, but rising more steeply near the origin as indicated by the ratios z/z^*. The integral may be calculated from

$$\varphi=\frac{z}{z^*}\left[1+(z_\infty-1)\operatorname{erf}\frac{y}{\sqrt{z_\infty}}\right]\varphi_0 \tag{17}$$

From equation (5), the heat flux through the gas is

$$q=-\frac{\varphi_0}{\sqrt{4a_0t}}\frac{dz}{dy} \tag{18a}$$

or in terms of the normalizing function z^*

$$q=-\frac{\varphi_0}{\sqrt{\pi a_\infty t}}\left(\frac{dz}{dz^*}\right)(z_\infty-1)\exp\left(-\frac{y^2}{z_\infty}\right) \tag{18b}$$

Figure 1(b) shows the ratio dz/dz^* as a function of w for various values of z_∞. The curves show how the heat flux varies throughout a gas in comparison with the first derivative of the error function.

The first derivative of z may be thought of as a normalized dimensionless heat flux (see eq. 18(a)). The value of this normalized heat flux at the boundary determines the value of z_∞ (see table I). The quantity z_∞^* will be defined as the limiting value which z would approach, for the given boundary derivative, if the thermal diffusivity were constant; that is,

$$z_\infty^*=1+\sqrt{\frac{\pi}{4}}\left(\frac{dz}{dy}\right)_0 \tag{19}$$

Figure 1(c) shows the ratio z_∞/z_∞^* as a function of $(dz/dy)_0$. It will be noted that z_∞/z_∞^* approaches a linear function of $(dz/dy)_0$ as the derivative increases.

HEAT CONDUCTION THROUGH CHEMICALLY REACTIVE GASES

The results obtained so far are for inert gases. Where the gas is chemically active and in local equilibrium, Hirschfelder (ref. 6) shows that the heat transferred by diffusion of reacting molecules and atoms results in increased thermal conductivity. If the heat of reaction is large, the coefficient of thermal conductivity becomes much larger than normal and goes through a pronounced maximum in the interval of temperature where the chemical reaction occurs. The thermal diffusivity, on the other hand, is not greatly affected by the reaction because the increase in thermal conductivity is compensated by a proportional increase in the specific heat As a result, the integral φ increases very rapidly with temperature compared to the diffusivity. Considered as a function of φ, the diffusivity is approximately constant during the interval of temperature where the coefficient of thermal conductivity is greatly increased due to the chemical reaction.

The diffusivity is most nearly independent of φ where φ increases most rapidly with temperature, that is, where the coefficient of thermal conductivity is a maximum. The temperature T_c where this maximum occurs is approximately the temperature where the specific heat is a maximum, or where the equilibrium mol fractions of the reacting species change most rapidly with temperature. The value of T_c may be calculated more precisely from equations derived by Butler and Brokaw for the coefficient of thermal conductivity (ref. 11)

$$k\simeq\frac{R\left(T\dfrac{d\ln K_p}{dT}\right)^2}{\sum\limits_j\sum\limits_i\dfrac{b_i}{nx_iD_{ij}}(b_ix_j-b_jx_i)} \tag{20}$$

where K_p is the chemical equilibrium constant in terms of partial pressures, n is the number of mols per unit volume, the x_i are the mol fractions of the ith component, and the b_i are the stoichiometric coefficients for the reacting components B_i when the chemical equation is written in the form

$$\sum_i b_iB_i=0 \tag{21}$$

For most common gases in the equilibrium state, these quantities are all precisely known functions of temperature. The binary mass diffusion coefficients D_{ij} are not so well known, in general, but they are relatively slowly varying functions of temperature and do not strongly influence the position of the maximum in k. Any reason-

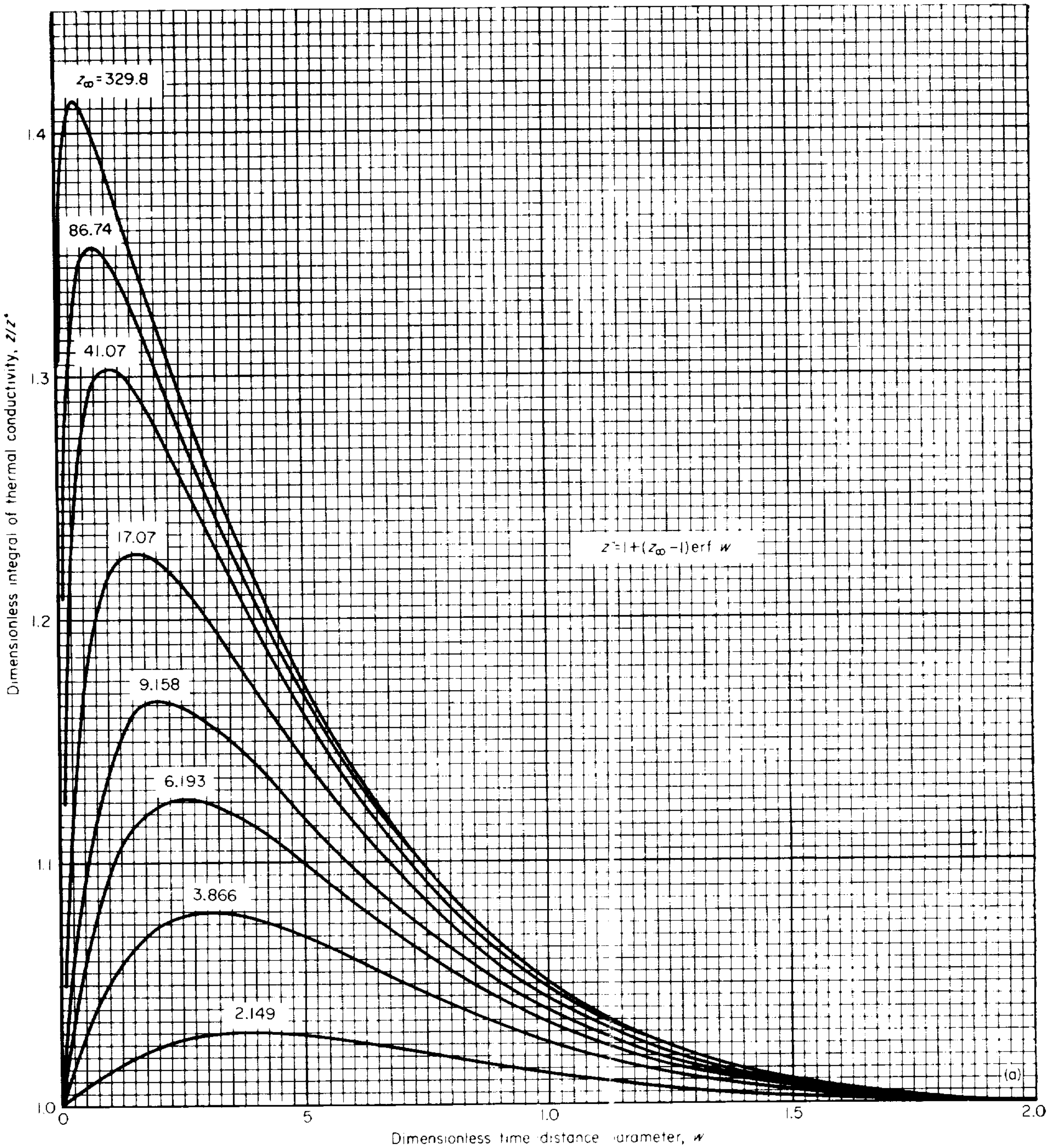

(a) Integral of thermal conductivity as a function of distance and time.

FIGURE 1. One-dimensional heat flow through an ideal gas where the initial temperature and boundary temperature are constants.

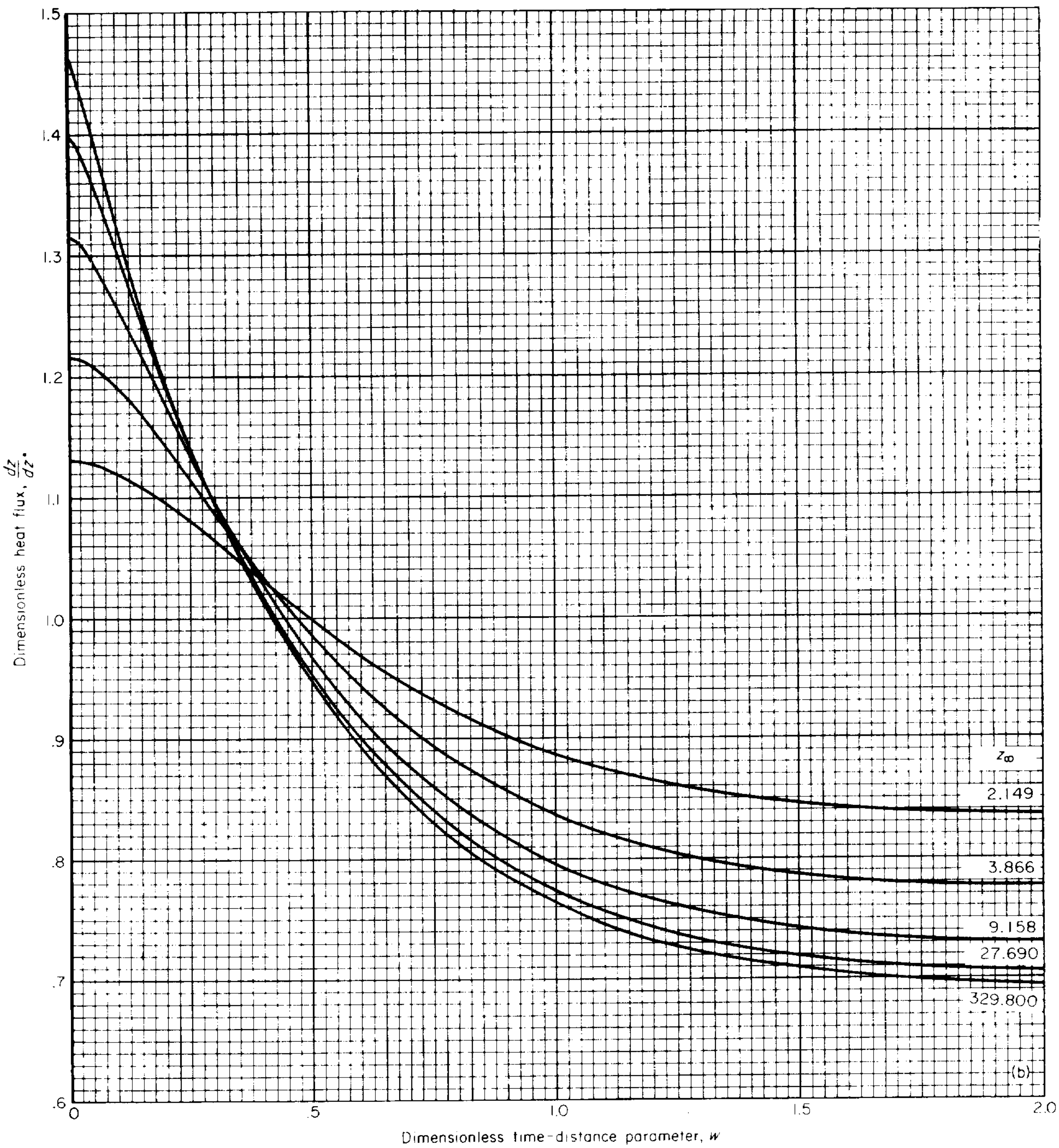

(b Heat flux as a function of distance and time.

FIGURE 1.—Continued.

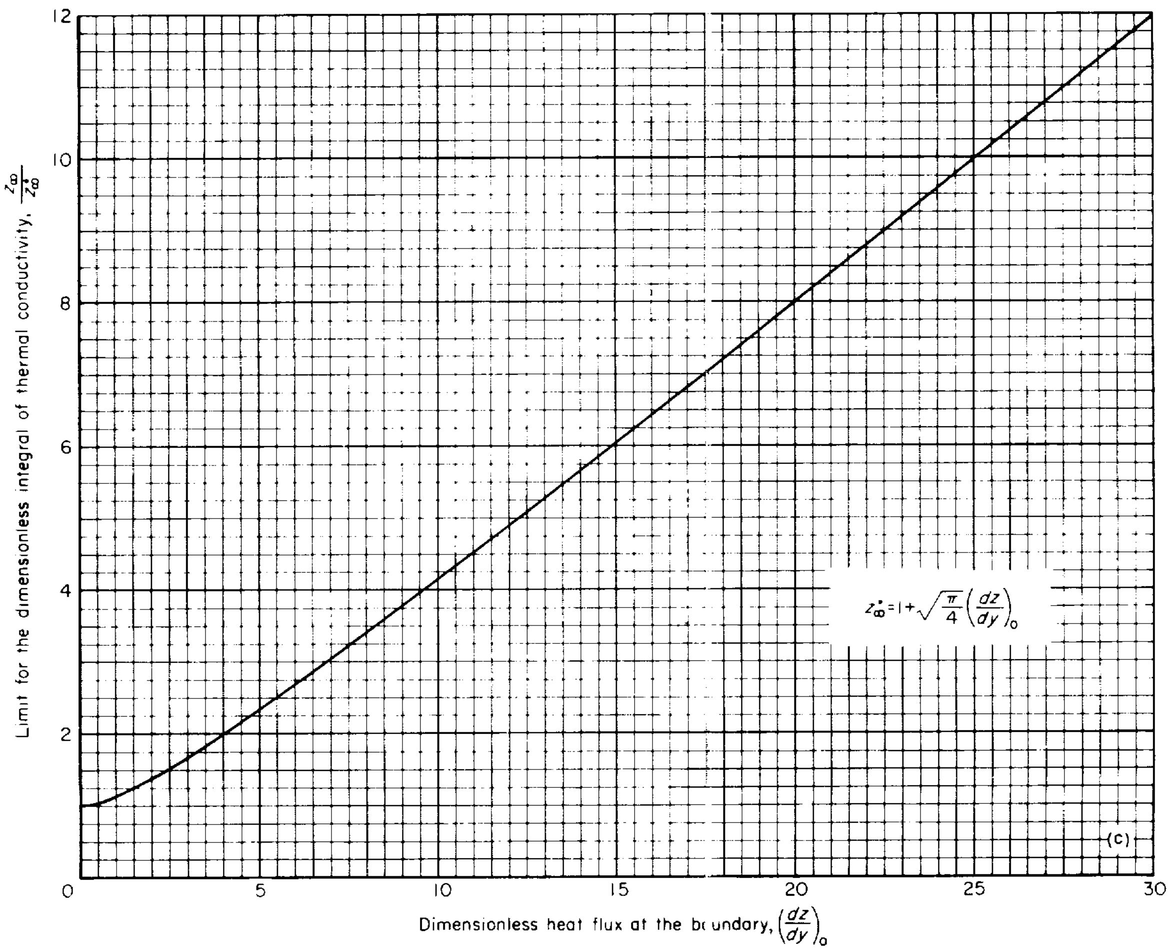

(c) Limit for the integral of thermal conductivity as a function of the boundary heat flux.

FIGURE 1.—Concluded.

able approximation for the mass diffusion coefficients will suffice for the calculation of T_c.

In the approximations which follow, it is assumed that a is proportional to ϕ up to the temperature T_c, above which it is a constant a_c. Once the boundary temperature T_0 is chosen, the value of z at the transition point is given by

$$z_c=\left(\frac{T_c}{T_0}\right)^{n+1} \tag{22}$$

The numerical integration of equation (14) is terminated at the point where z reaches z_c. This point uniquely determines values for the argument y_c and the derivative $(dz/dy)_c$. Since the diffusivity is assumed to be constant for $z>z_c$, the solution can be continued analytically to yield

$$z=z_c-\sqrt{\frac{\pi z_c}{4}}\left(\frac{dz}{dy}\right)_c\left(\exp\frac{y_c^2}{z_c}\right)\left(\text{erf}\frac{y}{\sqrt{z_c}}-\text{erf}\frac{y_c}{\sqrt{z_c}}\right) \tag{23}$$

The value of z_∞ is easily found from equation (23) by letting y go to infinity. Figure 2 shows the ratio z_∞/z_∞^* for chemically reacting gases as a function of the derivative $(dz/dy)_0$. Again, z_∞^* is given by equation (19). Curves are shown for z_c equal to 10, 20, 30, 40, 50, and 60. One can interpolate between these curves for the specific value of z_c given by equation (22), depending on the boundary condition and the chemical reaction considered. The dashed curve shows the inert-gas solution from figure 1(c) for comparison.

To illustrate an application of the above analysis, consider the case of air in which oxygen dis-

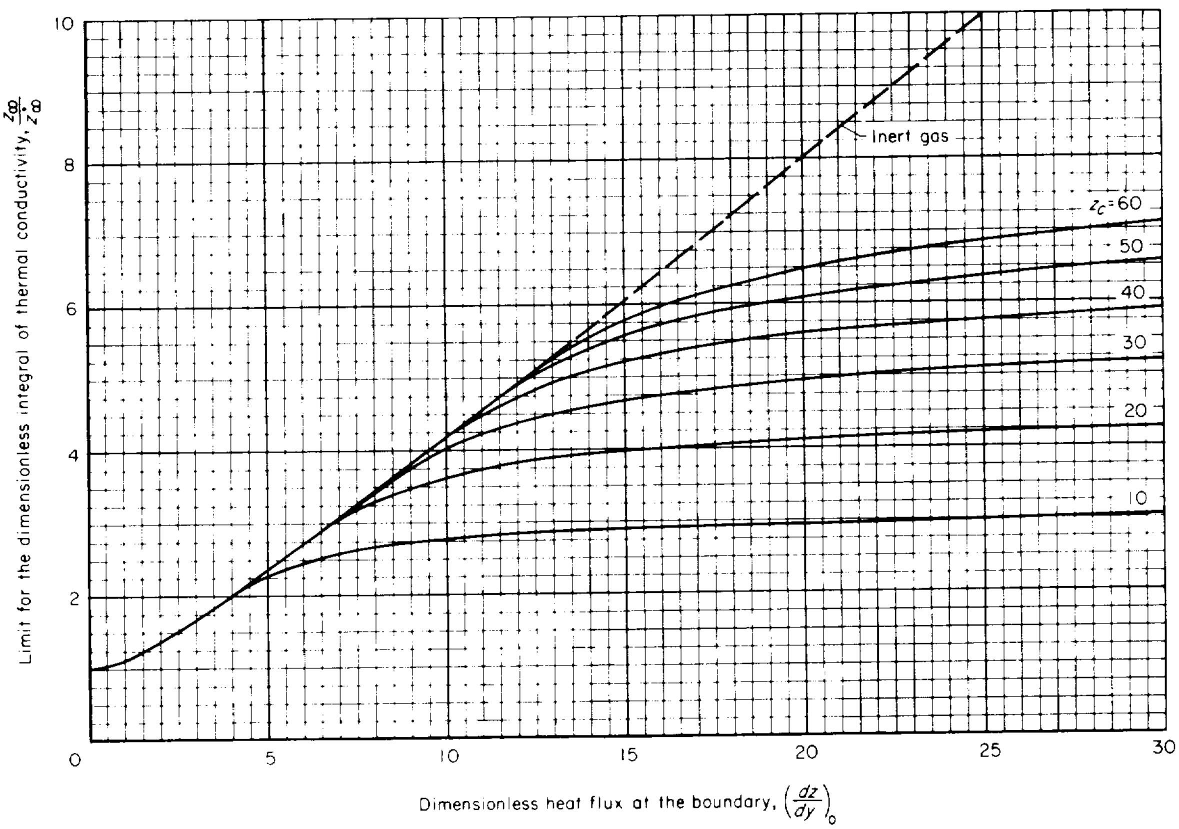

FIGURE 2. Integral of thermal conductivity as a function of boundary heat flux for a chemically reacting gas with large heat of reaction.

sociation can occur. The temperature T_c for this case is shown as a function of pressure in figure 3. The exponent n approaches a value of about 1/2 for high temperature air. Then if the boundary temperature is taken to be 293° K, z_c takes the values 21.3, 24.9, 29.6, 35.3, 42.2, 50.5, and 60.0 for air pressures of 0.0001, 0.001, 0.01, 0.1, 1.0, 10, and 100 atmospheres, respectively. Oxygen dissociation occurs at lower temperatures when pressure is decreased. Thus, the lower the pressure, the smaller the value of z_c, and the smaller the value of z_∞ which results in a given heat flux at the boundary (see fig. 2). Similarly, z_c is decreased when the boundary temperature is increased (eq. (22)) and again smaller values of z_∞ are required to produce a given slope $(dz/dy)_0$.

The functional relation between diffusivity and the integral φ is shown for air in figure 4. The ordinate and abscissa are normalized by the factors $z_c a_0$ and $z_c \varphi_0$, respectively, so that the relation becomes independent of pressure. The solid line on the figure shows the function assumed in the integration of equation (12). The dashed curve shows a theoretical estimate of the actual function based on the transport coefficients for air which are given in reference 12. This relation does not depend strongly on numerical accuracy of the coefficients. Thus, the exact function is probably not greatly different from the estimate, even though the latter is based on elementary kinetic theory and very approximate collision cross sections. It will be noted that the theoretical diffusivity is somewhat smaller than the assumed value in the interval where dissociation first begins, but is larger in the interval where oxygen dissociation nears completion. These errors tend to be averaged out by the integration process. When the oxygen dissociation becomes complete, the diffusivity again increases rapidly with φ, and the present solution loses validity. The splitting of the dashed curve in figure 4 indicates that the normalization factors $z_c a_0$ and $z_c \varphi_0$ do not remove the pressure dependence of this point.

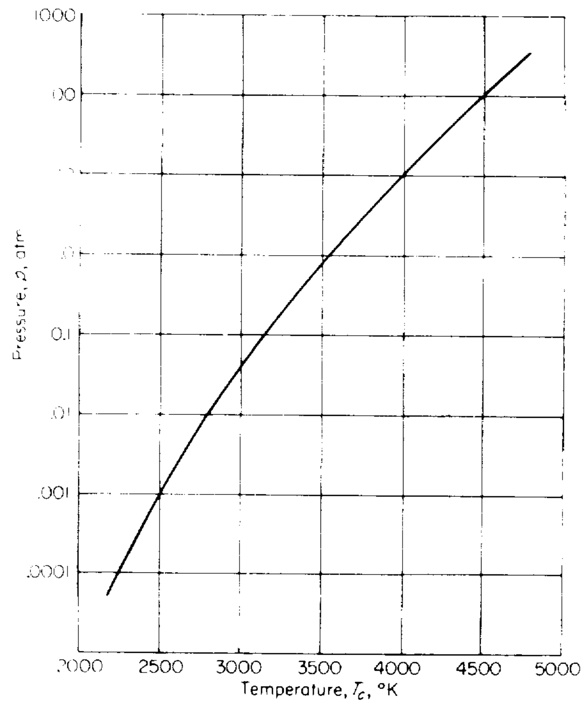

FIGURE 3.—Pressure and temperature conditions in air at which oxygen dissociation is responsible for a maximum in the coefficient of thermal conductivity.

HEAT CONDUCTION BETWEEN TWO SEMI-INFINITE MEDIA WITH UNIFORM INITIAL CONDITIONS

The foregoing results apply to the heat conduction through a semi-infinite gas medium with a constant boundary temperature. Such a condition is approximately satisfied where the gas is bounded by a thick wall of a metal which has a very large thermal conductivity and heat capacity per unit volume compared to the gas. In this case, the temperature change in the metal is small compared to the temperature change through the thermal diffusion layer of the gas, and the metal behaves essentially as an infinite heat reservoir at nearly constant temperature. Thus, the solutions given in the previous sections apply directly to such a case.

It is important to inquire now whether the solutions for the constant boundary condition will also apply to the nonsteady heat conduction through a gas bounded by a medium with arbitrary characteristics. The second medium might be an insulating type material or another gas at a different initial temperature, for example. It is instructive to recall first the case of the sudden thermal contact between two media with constant coefficients of thermal conductivity and diffusion and uniform initial conditions. Mersman, Berggren, and Boelter (ref. 13) show rigorously that the temperature at the interface between the two media comes instantly to a constant value, independent of time. It can be shown analytically that the same result applies where thermal conductivity is an arbitrary function of temperature, provided the thermal diffusivity is constant in each medium. In the case of gases, the diffusivity is not constant and the solutions are not in analytic form amenable to a general solution for the interface temperature. However, it can be seen that a particular constant value of the temperature T_0 will just balance the heat flux between the two media for all values of time t. Note that the heat flux at the boundary of a gas, with constant boundary condition φ_0, varies inversely as the square root of time,

$$q_0=-\left(\frac{\partial\varphi}{\partial x}\right)_0=-\frac{\varphi_0}{\sqrt{4a_0t}}\left(\frac{dz}{dy}\right)_0 \tag{24}$$

since the derivative $(dz/dy)_0$ is a function only of φ_∞ and φ_0 (see fig. 2), and is independent of time. By definition, the constant value of φ_0 implies a constant boundary temperature, T_0. Consequently, T_0 can always be adjusted to a particular constant value which will satisfy given uniform initial conditions in two adjoining semi-infinite media as well as continuity of heat flux beween the two media.

Consider now the case where the wall is a solid having constant coefficients of thermal conductivity k_s and of diffusivity a_s. Equating the heat fluxes at the boundary, one obtains

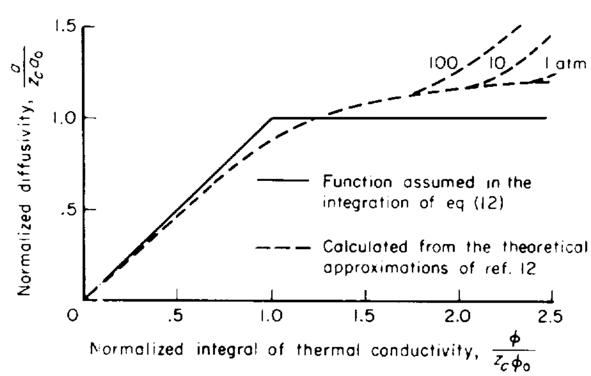

FIGURE 4.—Diffusivity for air as a function of the thermal conductivity integral.

$$\frac{\varphi_0}{\sqrt{4a_0t}}\left(\frac{dz}{dy}\right)_0=\frac{k_s(T_0-T_s)}{\sqrt{\pi a_s t}} \tag{25}$$

where T_s is the initial temperature of the solid. This result suggests a method of combining the analysis of nonsteady heat conduction through a gas with some experimental measurements for the purpose of determining the conductivity integral φ as a function of temperature. A shock wave reflected from the closed end of a tube can be used to create a layer of gas with essentially zero flow and constant, high-temperature initial conditions. Such an arrangement has been used by Smiley, for example, for making measurements of thermal conductivity in high-temperature argon (ref. 14). Assuming equilibrium, one can calculate the temperature of the shock heated gas from measured shock velocity or pressure. Then, if the temperature at the surface of the shock-tube wall is measured, and the thermal coefficients of the wall material and of the gas at low temperature are known, the normalized heat flux at the boundary $(dz/dy)_0$ may be evaluated from equation (25). This derivative uniquely determines the value of z_∞ upon integration of equation (12), or alternatively z_∞ may be evaluated graphically from the solutions plotted in figure 2. Thus the integral φ_∞ is determined as a function of T_∞, the initial temperature of the shock heated gas. The subsequent sections of this report will discuss such experiments performed to determine some values of φ for air.

EXPERIMENT

SHOCK-TUBE APPARATUS

The shock tube which was used to produce high-temperature air for the heat-conduction measurements is illustrated in figure 5. The tube consists of a cylindrical steel pipe, 2½-inches inside diameter and 22 feet long. The reservoir chamber is separated from the shock tube by a copper diaphragm. The diaphragm is ruptured when desired by a spring driven punch. The pyramidal tip of the punch cuts the diaphragm so that it tears into four equal leaves which fold back against the tube as shown in figure 5(c). In order to assure a clean rupture it is necessary to choose the thickness of the diaphragm so that it is stressed to about 85 percent of its yield strength under the pressure of the reservoir gas. After the rupture, the reservoir gas flows into the tube forming a shock wave in the gas with which the tube is initially filled.

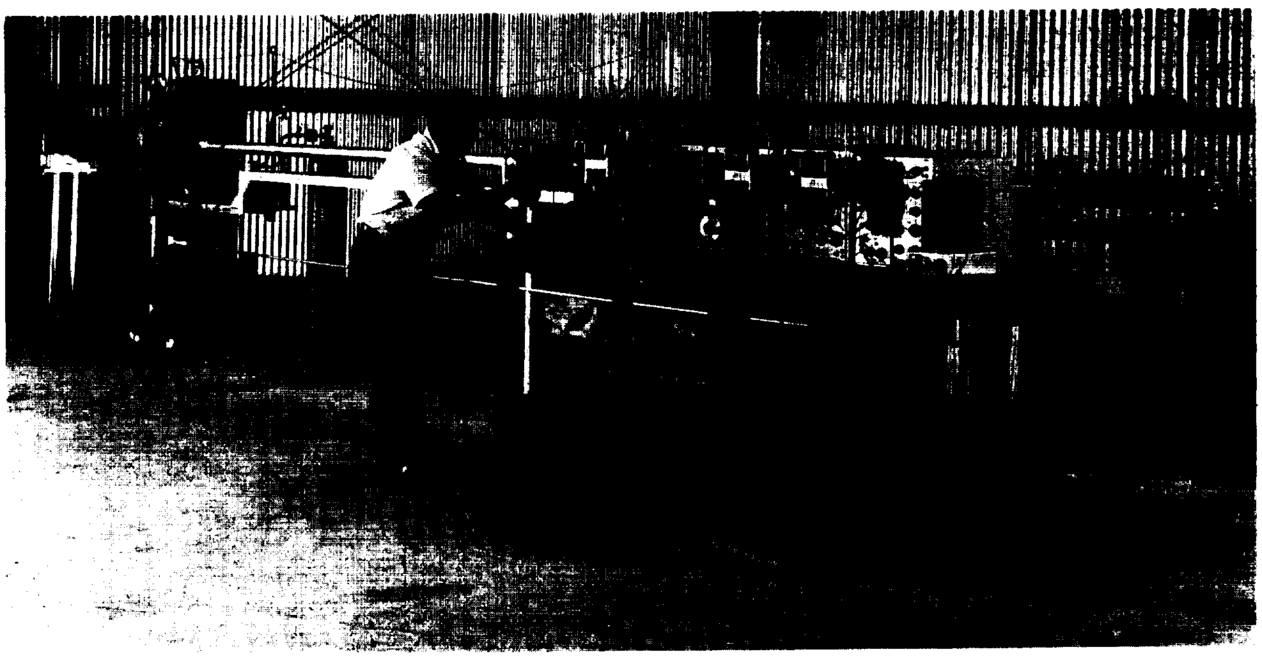

(a) Photograph of shock tube.

FIGURE 5.—Shock-tube apparatus.

Helium is used for the reservoir gas since it has a low molecular weight and the maximum ratio of specific heats. Because of these properties, strong shock waves are produced with moderate reservoir pressures (see, for example, the shock-tube equations in ref. 15). In addition, the reservoir is made large enough to function essentially as an infinite chamber in order to maximize the shock strengths obtained. This also serves to reduce the strength of those expansion waves, which propagate back into the reservoir, to a negligible amount. Thus, these expansion waves do not limit the interval of steady test conditions.

After the shock wave reflects from the end of the tube, the high-temperature air produced is in a steady-state condition, except for possible nonequilibrium effects. At the temperature and pressure conditions produced for the present experiments, the chemical relaxation times appear to be shorter than the available test interval (see appendix A), and it will be assumed here that the air is in equilibrium. The steady-state interval persists until disturbances arrive, several hundred microseconds later, due to the interaction between the reflected shock wave and the air-helium interface.

A distance-time diagram of the wave patterns in the shock tube is shown in figure 5(c) for convenience in establishing notation. The initial conditions are designated by a subscript 1; conditions following the initial shock wave are identified by subscript 2; and conditions following the reflection of the shock wave from the end of the tube are denoted by subscript 3. The initial conditions in the reservoir are assigned the subscript 4.

It is possible to calculate all of the equilibrium thermodynamic properties of the gases in regions 2 and 3 as a function of the initial gas temperature and pressure, T_1 and p_1, and the speed u_1 with which the shock wave propagates into region 1. Table II lists the nominal values for T_1 and p_1, which were used for the present tests, and the shock-wave Mach number M_1, which is obtained when helium at 34 atmospheres and normal temperature is used in the reservoir. The calculated pressures, temperatures, and densities of the air in region 3 (p_3, T_3, and ρ_3) are given. These are taken from the graphs presented in reference 16. The table also shows the calculated interval of steady conditions in region 3 and the relaxation times for the vibrational excitation of nitrogen molecules and for the dissociation of oxygen molecules. These are discussed further in appendix A.

CALIBRATION MEASUREMENTS

The initial pressure of air in the shock tube, p_1, was measured with a resolution of about ± 0.1 mm Hg. The initial temperature, T_1, was measured within 0.5° C. The shock Mach number, M_1, was determined by measuring the time interval required for the shock wave to travel between two pressure detectors mounted 18 inches apart in the side wall near the end of the shock tube (stations 1 and 5 shown in figs. 5(b) and 5(d)). The pressure detectors were piezoelectric barium titanate crystals embedded in an epoxyresin. The electrical output from the crystals was used to start and stop an electronic chronograph having a resolution of 0.1 micro-

TABLE II.—NOMINAL SHOCK TUBE OPERATING CONDITIONS: INITIAL TEMPERATURE, T_1 = 293° K; INITIAL HELIUM RESERVOIR PRESSURE, p_4 = 34 ATM

Initial air pressure, p_1, atm	Shock-wave Mach number M_1	Final equilibrium pressure, p_3, atm	Final equilibrium density ρ_3, Amagats	Final equilibrium temperature, T_3, ° K	Theoretical test interval Δt, μsec	N_2 vibrational relaxation time, μsec	O_2 dissociation relaxation time, μsec
1.00	3.0	52.6	11.15	1260	1470	8	----
.50	3.5	40.3	6.76	1580	1120	5	----
.25	4.1	33.2	4.06	2020	860	3	----
.125	4.7	21.9	2.36	2510	695	2	16
.062	5.4	15.3	1.35	3050	590	1.5	9
.031	6.0	10.0	.78	3420	495	1.5	9
.016	6.6	6.58	.46	3680	435	2	11
.008	7.2	4.20	.27	3840	370	3	16
.004	7.7	2.58	.15	4090	325	4	22
.002	8.2	1.58	.08	4440	275	5	29

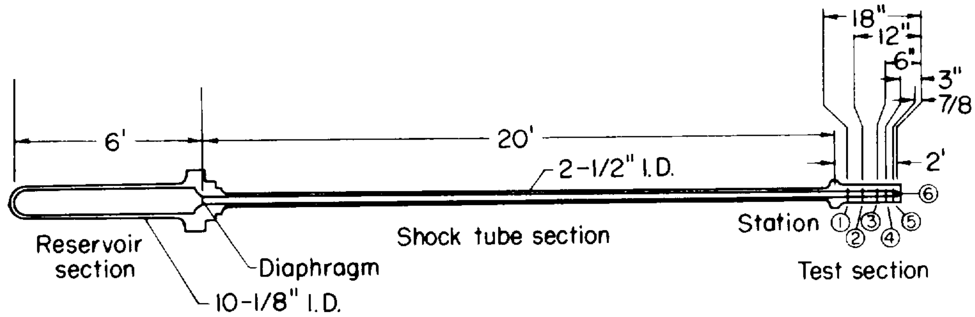

(b)

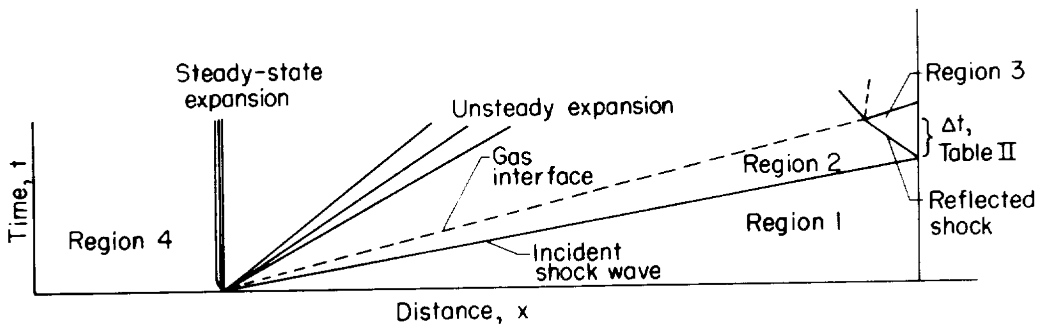

(c)

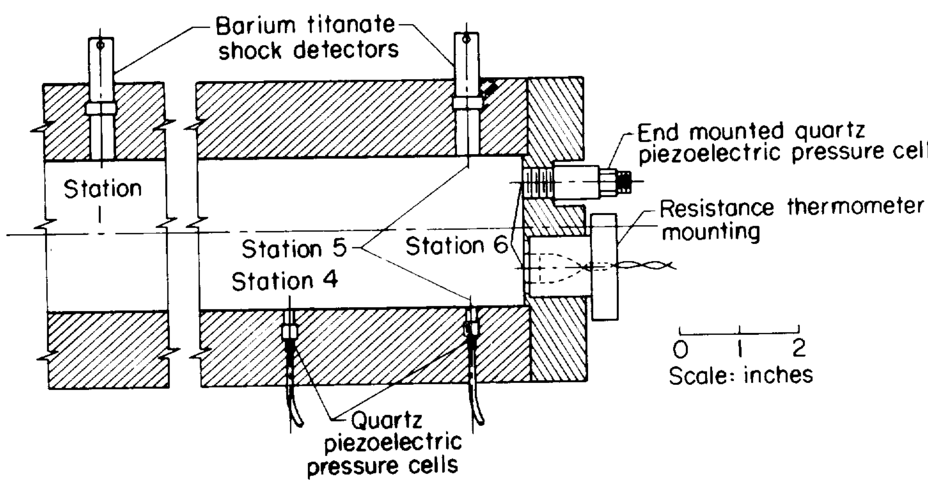

(d)

(b) Schematic diagram of shock tube.
(c) Time-distance wave diagram for shock tube flow.
(d) Schematic drawing of shock tube test section.

FIGURE 5.—Continued.

second. The actual resolution of the pressure pulse was limited by the resonant frequency (20 kc) and the size (0.3-inch diameter) of the detector. However, the counter start and stop channels were set to trigger at the same part of the output wave form so that delays in the response of the two detectors compensated each other. In this way a resolution of about 1 microsecond is obtained in the measured time interval, and the velocity is given with a probable accuracy better than 1 percent. The Mach number M_1 is simply the measured velocity u_1, divided by the speed of sound in air at temperature T_1.

It is desirable to check the calculated properties of the shock heated air with experiment. For this purpose, the pressures p_2 and p_3 were measured with a quartz piezoelectric crystal detector having a diameter of 0.15 inch and a frequency response from essentially d.c. to 100 kc. The output from the crystal was recorded with an oscilloscope-camera combination. The d.c. characteristics were maintained by matching the high internal impedance of the detector (more than 100,000 megohms), through an electrometer tube, to the input impedance of the oscilloscope. Figure 5(f) shows a view of the detector housings and figure 5(g) shows the impedance matching unit and oscilloscope. The detectors were mounted flush with the side wall of the shock tube in order to measure p_2. Some typical pressure records from

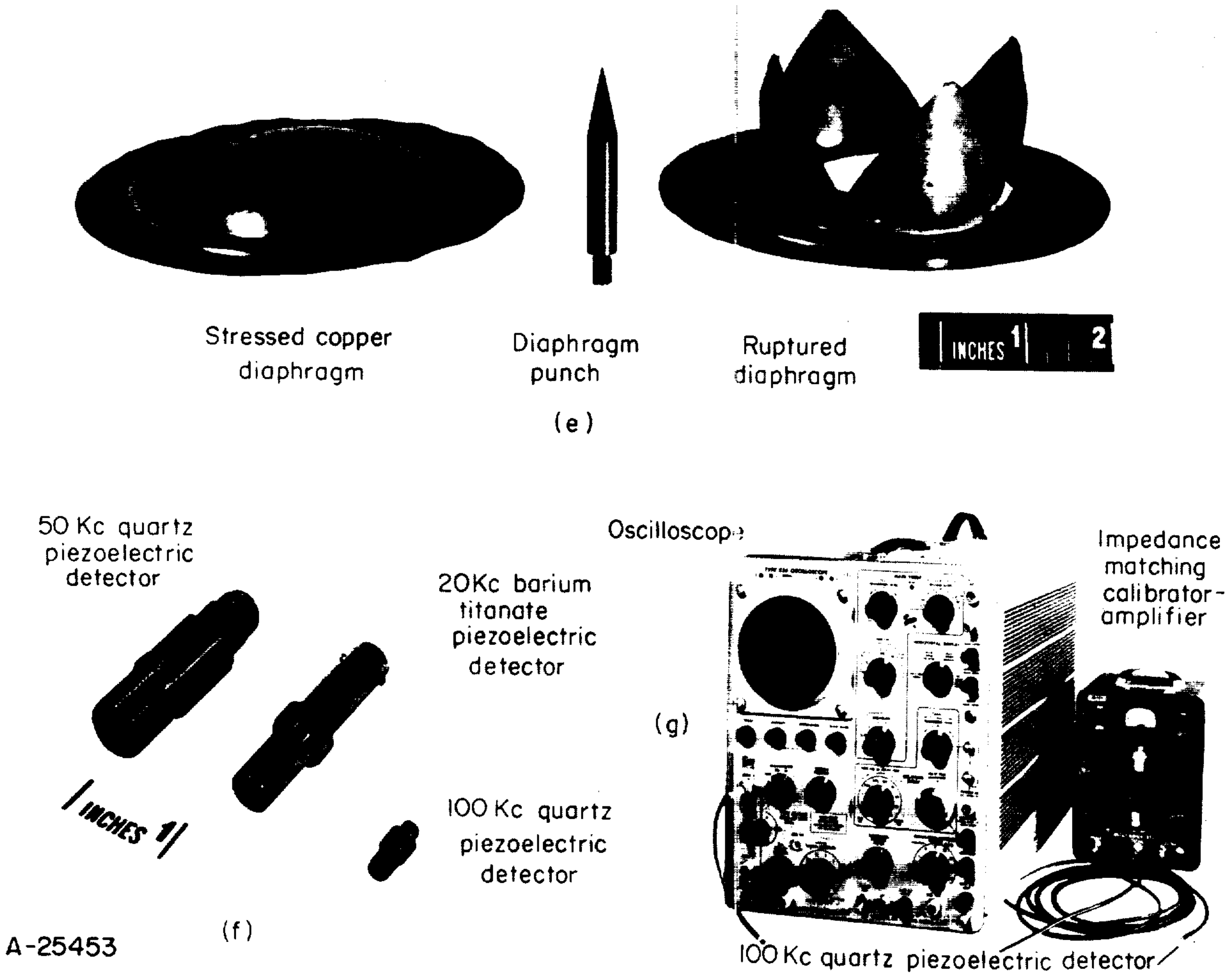

(e) Diaphragms.
(f) Pressure cells.
(g) Calibrating and recording equipment.

FIGURE 5.—Concluded.

the side wall mounted gage are shown for a number of different shock speeds in figures 6(a) through 6(c). The pressure jumps from p_1 to p_2 when the initial shock wave passes, and then later jumps to p_3 when the reflected shock arrives. (See sketch (a).)

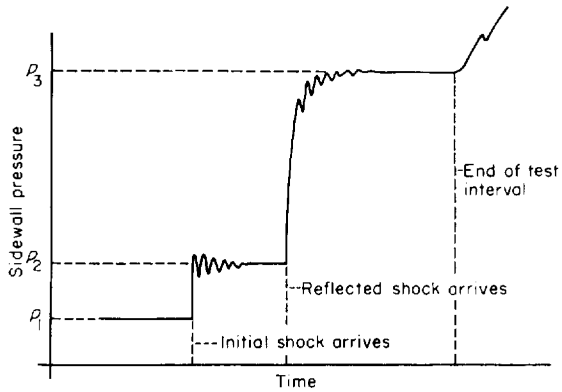

Sketch (a)

At higher shock strengths, some disturbances arrive at the side wall position ahead of the reflected shock, apparently through the boundary layer. This effect can be seen in figure 6(c), for example. In order to avoid this effect above Mach number 5.5, the pressure p_3 was measured with the detector mounted at station 6 in the end cap of the shock tube. A larger quartz piezoelectric pressure detector with a 50 kc resonant frequency was used at this station. The spurious side wall effects were absent at station 6 as shown in figures 6(d) and 6(e). The oscillations on all the pressure records are due to excitation of the lowest resonant frequency of the pressure pickups. These have been averaged out in determining the pressures from the records. Due to this factor and the other irregularities, uncertainties in measured pressures are the order of 10 percent.

Figure 7(a) shows the pressure p_2 as a function of the theoretical p_2 corresponding to the measured Mach number M_1. The agreement is reasonably satisfactory in view of the uncertainty in the data. Figure 7(b) shows the measured pressure p_3 as a function of the calculated values for p_3. Again the agreement is within the order of accuracy of the measurements. The value of p_3 is considerably more sensitive to nonequilibrium effects than is p_2 (see ref. 16), and so the comparison shown in figure 7(b) indicates that the air reaches a state close to equilibrium.

TEMPERATURE MEASUREMENTS

A temperature detecting instrument was mounted flush with the wall in the end cap of the shock tube (fig. 5(d)). This instrument consisted of a pyrex cylinder with a film of nickel evaporated over part of the front face (fig. 8). The nickel films measured about 100-ohms resistance between contacts; the portion of the film responsible for this resistance was a thin strip of nickel about 1 cm long, 1 mm wide, and 900 Å thick. The film was connected as the active element in a d.c. bridge circuit. The resistance of the film was measured as a function of time by recording the output from the bridge circuit with oscilloscope-camera equipment. The resistance of the film is found to be a linear function of its temperature, which is taken to be the temperature of the pyrex surface (see appendix B). A typical temperature record indicated by this instrument is illustrated in sketch (b). Some of the actual records are

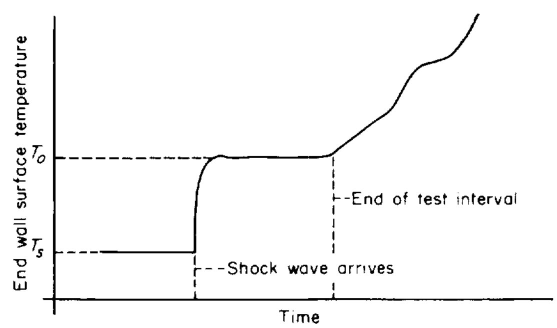

Sketch (b)

shown in figure 9 for a variety of shock wave speeds from Mach number 3.0 to 7.7. It can be seen that, to a first approximation, the temperature of the glass surface jumps to a constant value after the reflection of the normal shock wave. Some irregularities appear in the output at higher shock speeds, apparently due to pickup of electrical charge from the hot air. The effect has been limited in this case by coating the nickel film with a thin layer of silicon monoxide. A further discussion of this effect and a description of the preparation and calibration of the films is given in appendix B. The temperature measurements are reproducible to the order of ±20 percent.

Where the surface temperature jumps to a constant value, T_0, the heat flux into the wall can be calculated if the coefficients of thermal conductivity k_s and diffusivity a_s are both known

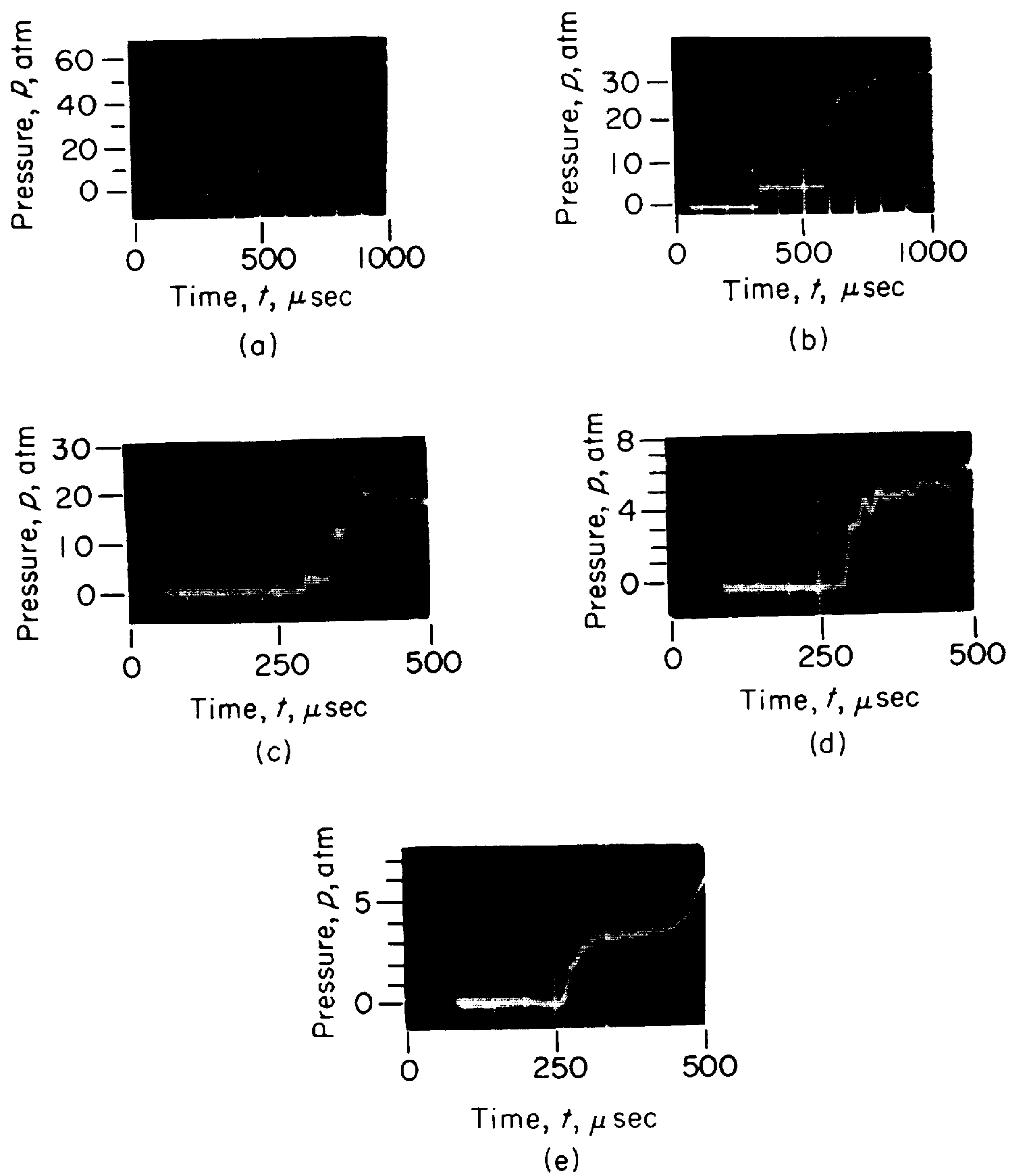

(a) $M_1=3.04$, $p_1=1.00$ atm, station 4. (b) $M_1=4.05$, $p_1=0.250$ atm, station 4.
(c) $M_1=5.44$, $p_1=0.062$ atm, station 5. (d) $M_1=6.72$, $p_1=0.016$ atm, station 6.
(e) $M_1=7.79$, $p_1=0.004$ atm, station 6.

FIGURE 6.—Shock-tube pressure records.

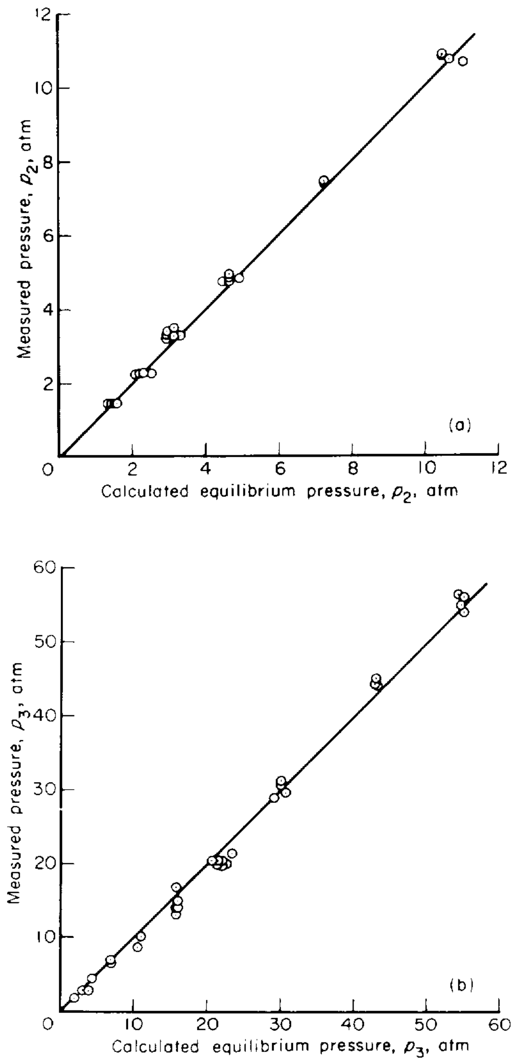

(a) Pressure of air following the normal shock wave.
(b) Pressure of air after reflection of the normal shock wave.

FIGURE 7.—Measured pressures in the shock tube as a function of calculated equilibrium pressures.

for the wall material (see eq. (25)). In the present experiments, the following values have been used for the thermal coefficients of pyrex

$$a_s = 0.0057 \text{ cm}^2/\text{sec} \tag{26a}$$

$$k_s = 0.0024 \text{ cal/cm deg sec} \tag{26b}$$

The diffusivity a_o and the integral of thermal conductivity φ_0 for the air at the wall are also a function of the measured surface temperature T_0. At moderate temperatures, such as obtained in the present experiments, these are approximately given by

$$\varphi_0 = 3.2 \times 10^{-6}\ T_0^{3/2} \text{ cal/cm sec} \tag{27a}$$

$$a_0 = 17.7\ (\varphi_0/p) \text{ cm}^2/\text{sec} \tag{27b}$$

where T_0 is in degrees Kelvin and p in atmospheres.

The quantities given by equations (26) and (27) permit the evaluation of the slope $(dz/dy)_0$ from the measured interface temperature T_0 (eq. (25)). Then the value of z_∞, and thus φ_∞, may be obtained from the solutions shown graphically in figure 2. Since the value of T_∞, or T_3, is known from the measured shock speed, the objective of the experiment is completed; that is, φ is evaluated as a function of T.

DISCUSSION OF RESULTS

The results from the experimental evaluation of φ as a function of T are shown in figure 10. The dependent variable is the ratio of φ to the value φ^* for idealized air with constant specific heat. The latter is given by

$$\varphi^* = 3.2 \times 10^{-6} T^{3/2} \text{ cal/cm sec} \tag{28}$$

where T is in degrees Kelvin. The ratio φ/φ^* is approximately unity as long as the air remains in the molecular state. The oxygen molecules begin to dissociate at about 2,500° K and φ becomes larger than its ideal value as a result of the increase in thermal conductivity caused by the dissociation reaction. As the temperature increases to the point where oxygen dissociation is nearly complete, φ becomes about 2½ times larger than its ideal gas value. The theoretical curve shown in figure 10 was computed from graphical integration of the coefficients of thermal conductivity presented in reference 12. The experimental values lie somewhat above the theoretical curve, but the difference is hardly more than the deviation in the experimental data. It should be noted that the function shown is for the particular progression of pressures obtained in the shock tube. Similar curves would be obtained at other pressure levels. For example, the theoretical values for φ are shown in figure 11 as functions of temperature up to 15,000° K and for constant pressures of 0.0001, 0.001, 0.01, 0.1, 1.0, 10 and 100 atmospheres. As temperature increases, the three distinct jumps in the value of φ are due to the dissociation of oxygen, the dis-

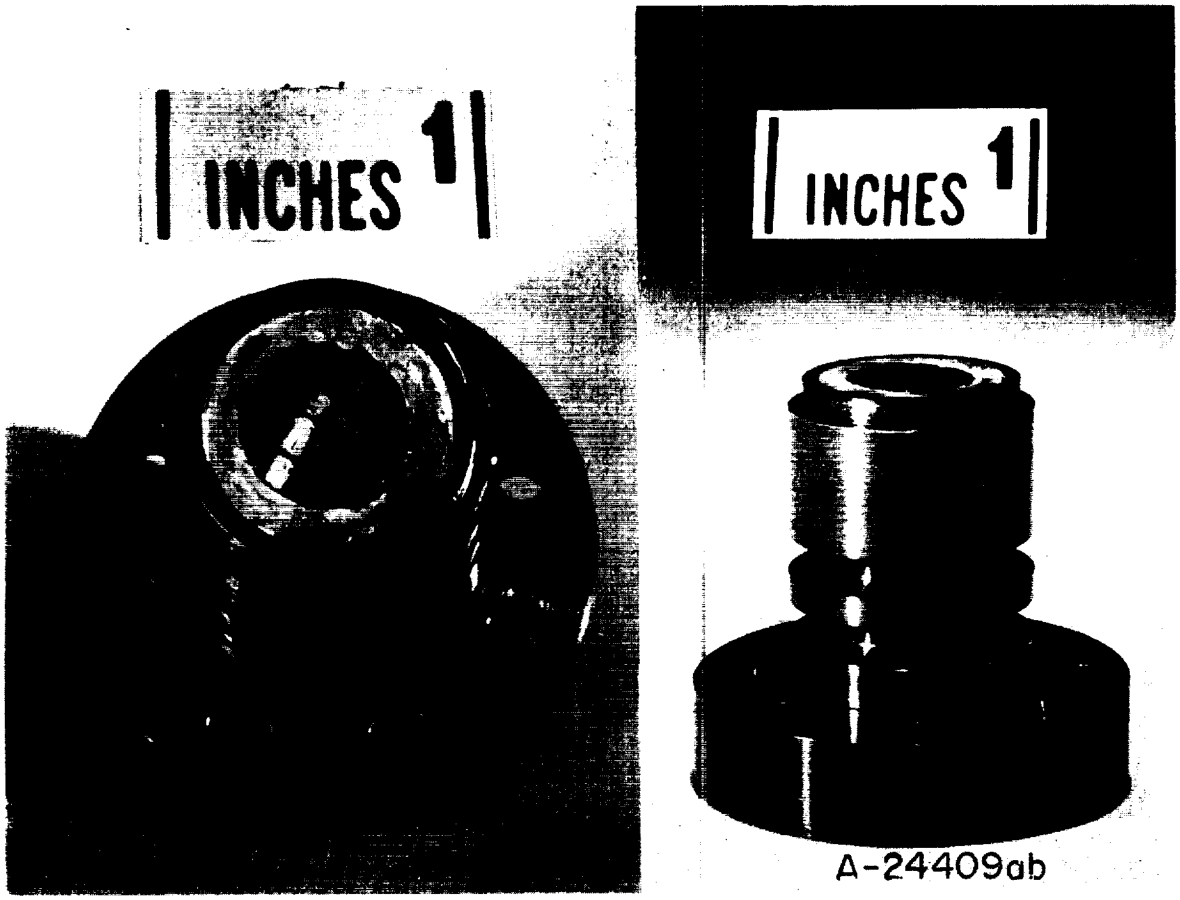

FIGURE 8.—Surface temperature detector.

sociation of nitrogen, and the single ionization of both oxygen and nitrogen atoms. Each of these reactions causes a large increase in the coefficient of thermal conductivity (refs. 6 and 12) and a corresponding increase in the integral, φ.

The experimental data suggest that the theoretical estimates of thermal conductivity for air, in which oxygen dissociation occurs, may be low by about 20 percent. Because of uncertainties in estimating collision cross sections (see ref. 12), a discrepancy of this magnitude in the theory is easily conceivable. The difference could also be caused by the presence of free electrons in excess of the concentrations predicted for pure air in equilibrium (ref. 17). According to reference 12, electron mol fractions the order of 10^{-3} would be sufficient to increase the calculated thermal conductivity to the level of the present experimental data. Such electron concentrations might result from small amounts of impurities in the shock-heated air. However, the inconsistencies in surface temperature measurements are at present responsible for deviations of the same magnitude as the difference between the experiment and the theoretical estimates. Therefore, more precise experimental data will be needed before it should be inferred that a significant difference does exist.

CONCLUDING REMARKS

In calculating the flow of heat through gases, it is important to consider the variation in the coefficients of thermal conductivity and diffusivity. The natural parameter which replaces temperature as the dependent variable in such calculations is the integral of thermal conductivity with temperature. With this choice of the dependent variable, the numerical integration of the one-dimensional heat-conduction equation is straightforward if the initial and boundary conditions are constants and if the coefficient of diffusivity is assumed to be a

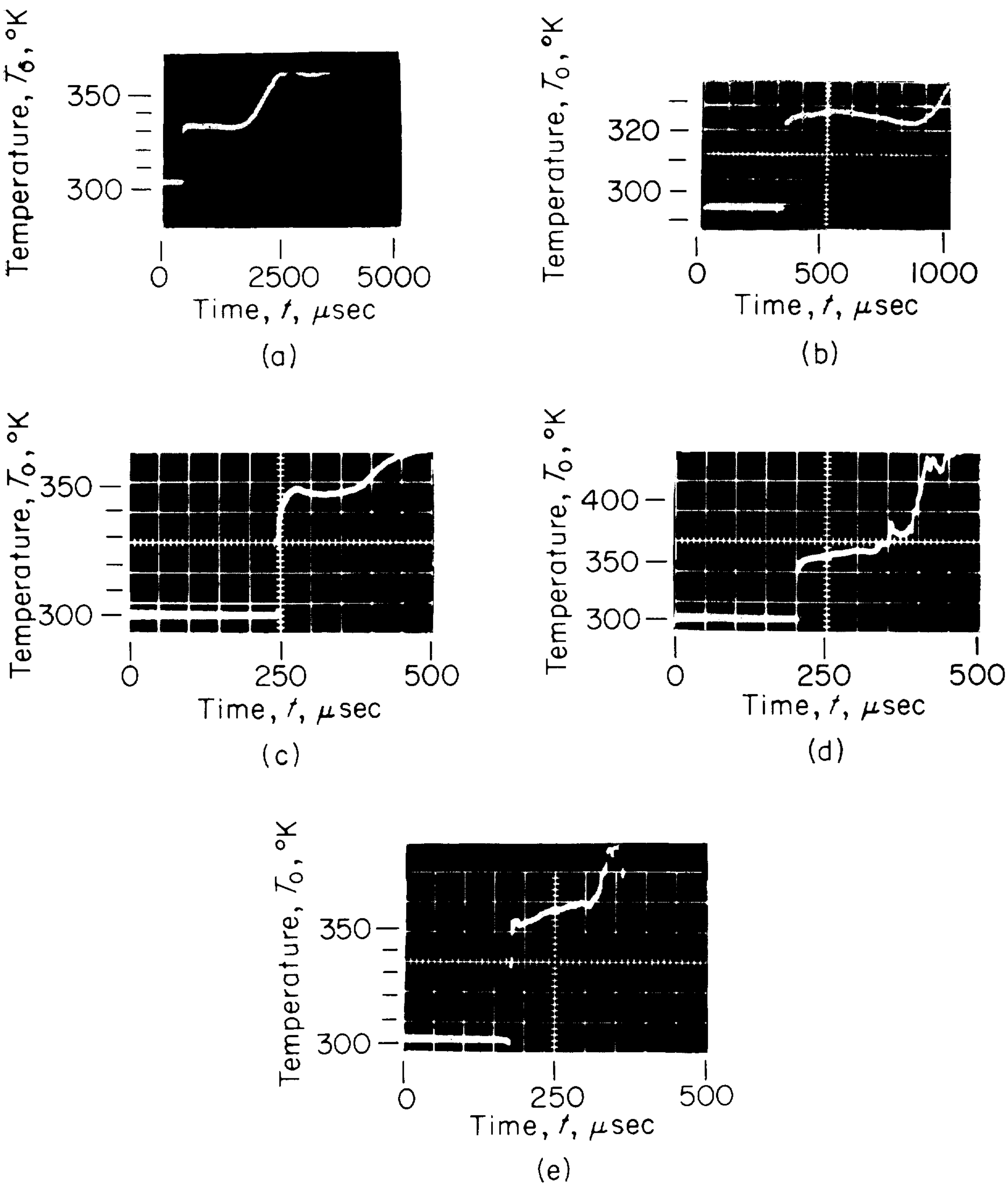

(a) $M_1=3.04$, $p_3=54.8$ atm, $T_3=1,290°$ K. (b) $M_1=4.05$, $p_3=30.4$ atm, $T_3=1,980°$ K.
(c) $M_1=5.44$, $p_3=18.0$ atm, $T_3=3,190°$ K. (d) $M_1=6.72$, $p_3=6.40$ atm, $T_3=3,810°$ K.
(e) $M_1=7.74$, $p_3=3.96$ atm, $T_3=4,240°$ K.

FIGURE 9.—Records of temperature at the surface of a pyrex slab at station 6.

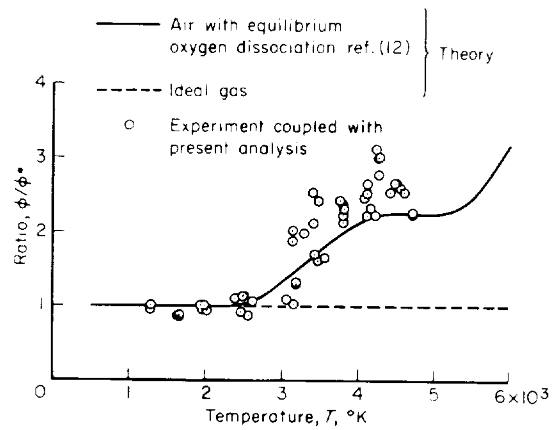

FIGURE 10.—Integral of thermal conductivity for air as a function of temperature; $\phi^*=(2/3)k_0T_0(T/T_0)^{3/2}$.

known function of the conductivity integral alone. For ideal gases, diffusivity is approximately proportional to the conductivity integral. Air can be treated as an ideal gas up to the point where oxygen dissociation becomes effective. Over the range of temperature where the oxygen dissociation occurs, it is reasonable to assume that diffusivity is independent of the conductivity integral. The solutions obtained in this way break down at temperatures where oxygen dissociation becomes complete.

The shock tube is an instrument which can produce a reservoir of high-temperature gas with approximately constant initial conditions. These initial conditions may be calculated from measurements of the shock velocity. Temperature measurements at the surface of a wall which reflects the shock wave can be used in conjunction with the solutions for heat conduction in the gas to evaluate the conductivity integral as a function of temperature. At the present stage of development, the experiments exhibit considerable variation, mainly because of uncertainty in the measurements of surface temperature. However, the experiments show the same functional behavior for the coefficient of thermal conductivity as predicted by theoretical estimates. The agreement between the experiment and theory is within the accuracy of the measurements and within the limits of uncertainty in theoretical calculations of transport properties.

AMES RESEARCH CENTER
NATIONAL AERONAUTICS AND SPACE ADMINISTRATION
MOFFETT FIELD, CALIF., *Feb. 27, 1959*

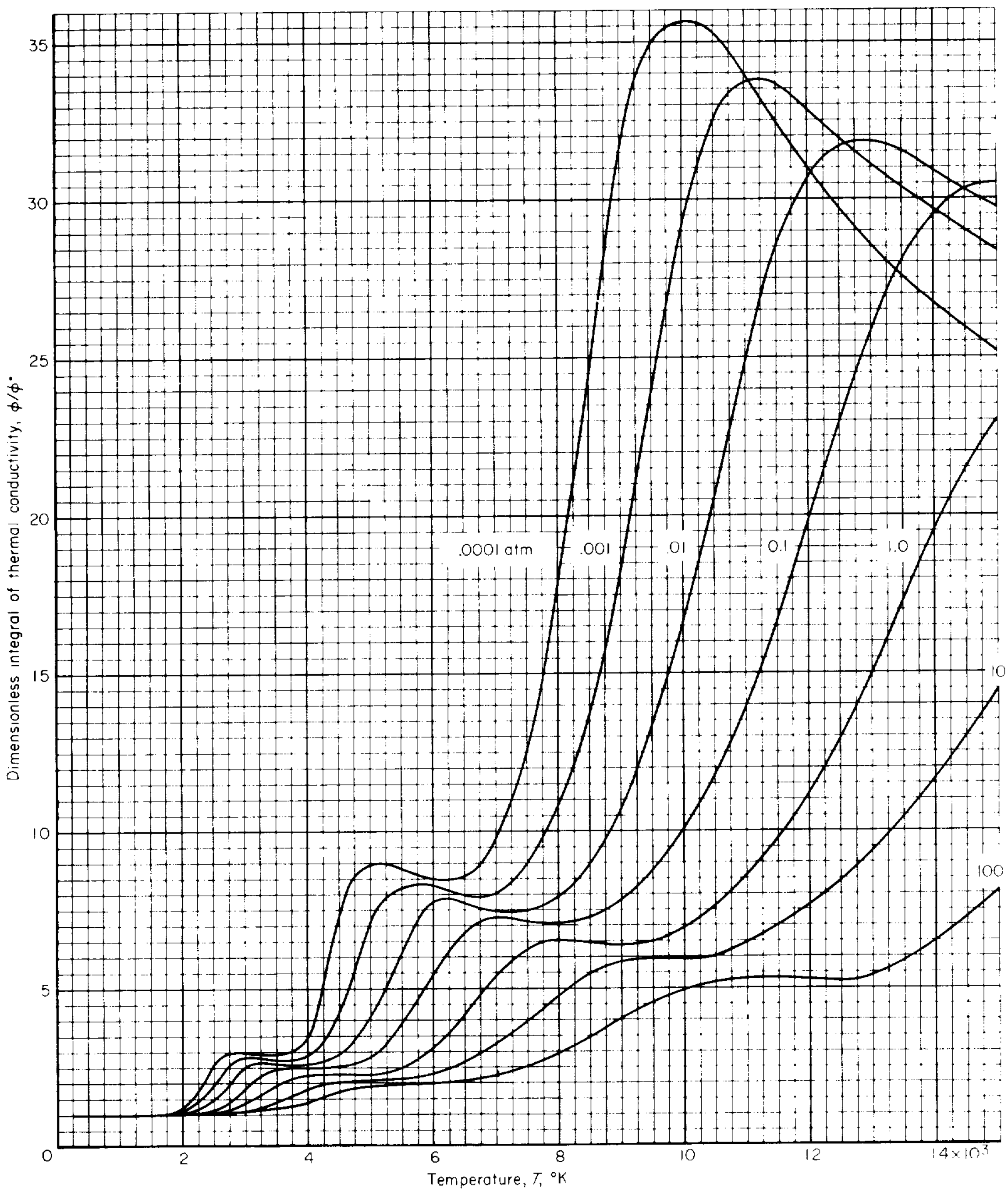

FIGURE 11.—Theoretical estimates for the integral of thermal conductivity for air; $\phi^* = (2/3)k_0T_0(T/T_0)^{3/2}$.

APPENDIX A

CHEMICAL RELAXATION IN SHOCK-HEATED AIR

It has been assumed in this report that the shock-heated air reaches instantaneous equilibrium. It is well known that actually a finite number of molecular or atomic collisions are required to produce the equilibrium partition of energy (ref. 18). Thus, the gas takes a finite time to relax to the steady-state condition. It is the purpose of this appendix to discuss the question whether the relaxation phenomena might affect the heat flux experiments in the shock tube.

At the temperatures and pressures encountered in the present experiments (see table II), the following modes of energy can be excited in air: the kinetic motion of molecules and atoms, the rotation of molecules, the vibration of molecules, and the dissociation of oxygen molecules into atoms. No more than a few collisions are required to produce the equilibrium distribution of kinetic and rotational energies. Thus, for practical purposes, the relaxation times for these modes of energy are negligible. Of concern, then, are the vibration of oxygen and nitrogen molecules and the dissociation of oxygen.

The vibrational relaxation times have been calculated for the present experiments using the measurements reported by Blackman (ref. 19). The relaxation times for oxygen molecule vibrations were very short, the order of a fraction of a microsecond. This interval is less than the time resolution of the instruments involved. Nitrogen molecule vibrational relaxation times were somewhat longer, the order of several microseconds, and these are listed in table II. Although the instruments might resolve these time increments, the relaxation times are still very short compared to the total test interval (the order of a hundred microseconds or more). In addition, the energy transfer involved in the excitation of nitrogen vibrations is at most 18 percent of the total enthalpy. Therefore, the assumption of equilibrium appears to be justified in this case.

In the case of oxygen dissociation, the energy transfer by the reaction is comparatively large, and the corresponding relaxation times appear to be somewhat longer than in the case of vibrational excitation. The oxygen dissociation relaxation times have been estimated from the experimental results of Camac, Camm, Keck, and Petty (ref. 20). These estimates range from 10 to 20 microseconds as shown in the last column of table II. These times are still somewhat shorter than the test interval, and the wall temperatures appear to approach a steady value. In addition, recall that the measured values for p_3 approach the calculated equilibrium values (fig. 7(b)). Thus the assumption of equilibrium may be a reasonably good first approximation.

A precise analysis of the shock reflection experiment would need to include consideration of dissociation relaxation. The gas near the wall would be at a higher initial temperature than the gas away from the wall, which would have time to approach the lower equilibrium temperatures before being influenced by the wall conditions. After the reflection of the shock wave, the gas near the wall will approach equilibrium at the same time it is cooled by heat conduction to the wall. The relaxation process is equivalent to having a heat sink in the gas. Thus the exact solution requires the calculation of heat conduction through a medium with variable coefficients and nonconstant initial conditions, and in the presence of a heat sink function distributed in time and space.

APPENDIX B

PREPARATION AND CALIBRATION OF NICKEL-FILM SURFACE TEMPERATURE DETECTORS

The instrument used to measure the temperature at the surface of the shock reflecting wall consisted of a thin strip of nickel evaporated onto a pyrex glass backing (fig. 8). Glass was chosen for the backing material because its surface temperature, resulting from heat conduction through the gas, would be higher than for most other solids. This is due to the fact that glass has a small value for the product $kC\rho$, and the interface temperature varies inversely as the square root of this product (see ref. 13). Physically, it can be seen that a material which conducts the heat away from the surface slowly and which has a small thermal capacity per unit volume will come to a comparatively high surface temperature. Nickel was used for the film resistance element because it is relatively easy to evaporate with high purity and it has a large coefficient of resistance change with temperature.

The nickel film is thin enough so that it is in equilibrium with the surface temperature of the glass. For example, if a film of thickness Δx is backed by a material having a lower value of $kC\rho$, the time τ for the average temperature of the film to come within 0.01 of a step input in temperature is limited by

$$\tau < \frac{(\Delta x)^2}{16a \times 10^{-4}}$$

where a is the diffusivity of the nickel (about 0.16 cm²/sec). Thus, for a film 900 Å thick, the time τ is less than 0.32 microsecond. This time is so short that the film essentially responds instantly to changes in the surface temperature.

The resistances of the films were calibrated as a function of temperature between 20° and 90° C by a static method. The film, the glass slab, and the mounting were placed in a container immersed in a water bath. Thermostats and heaters in the bath controlled the temperature in the container within 0.5° C. A thermocouple was imbedded in the metal mounting and another was placed in the air of the container about 2 mm directly above the nickel film. The calibration measurements were made after the output from these thermocouples agreed within 0.5° C. The thermal masses involved were such that about 5 minutes were required for the film mounting and the air within the container to reach equilibrium with the bath.

The resistance of the nickel films was measured using a standard bridge circuit and a potentiometer (in the shock-tube tests an oscilloscope-camera recorder replaced the potentiometer in order to achieve the time resolution required). It was found that if the nickel films were carefully prepared, the resistance was a linear function of temperature within the range from 20° to 90° C. The deviation of the calibration data from the least squares linear fit was about 1 percent. The temperature coefficient of resistivity, α, was computed from the slope, m, of the resistance versus temperature data divided by the reference value of resistance, R_0, at 20° C

$$\alpha = \frac{m}{R_0} \text{ or } \frac{R - R_0}{R_0(T - T_0)} \tag{B1}$$

It was found that the coefficient for the evaporated films was considerably smaller than the coefficient for bulk nickel. For example, the average value of α for 10 stable film instruments was 0.0017 per deg C, with the variation between films amounting to about 10 percent. In contrast to this, the coefficient for bulk nickel at 20° C is about 0.0043 per deg C (ref. 21). Rabinowicz, Jessey, and Bartsch (ref. 22) found that the same order of difference exists between the coefficients for platinum films and bulk platinum.

Several of the difficulties encountered in the preparation and use of the nickel films are noteworthy. First of all, the glass surface and the vacuum system in which it is placed must be clean before evaporation of the nickel is attempted. It was found, for example, that the nickel films could have a very nonlinear calibration where the

524300—60——4

vacuum system had been contaminated with pump oil or other organic vapors. Moreover, the calibration was not always stable, and the values of α were generally considerably lower than 0.0017 per deg C. The nickel used in the evaporation should be quite pure also, of course. According to reference 22 similar precautions are essential in the preparation of platinum films.

A second property of the nickel films which has been observed is that their calibration is not stable until the films have been baked at elevated temperature for an extended time. The films were baked at 180° C for about 16 hours. Generally this resulted in a film with stable characteristics and one which was considerably tougher than the unbaked film. No attempt was made to determine an optimum baking procedure.

When the films were used in the shock tube, they sometimes increased slightly in resistance after a test run. This might be due to erosion of the film by small particle bombardment. Evidence of such erosion could be seen on microscopic examination of the film. The resistance increase could also be associated with the rather large increase in film temperature after the test interval (see fig. 9). This increase in temperature is probably due to the reflection of shock waves from the helium interface and to the large increase in thermal conductivity and diffusivity of the hot air when it becomes mixed with small amounts of helium. Similar increases in film resistance were observed in a calibration cycle after overheating. Unless the film was permanently damaged, the increase in resistance was less than 2 percent, however. Films were calibrated both before and after a series of shock-tube runs, and it was found that the slope of resistance versus temperature was not affected by the change in the reference resistance. The value of α is a function of R_0, however (see eq. (B1)), and it was adjusted accordingly.

Finally, one more troublesome effect which occurred when the films were used in shock-heated air above 2,500° K was due to the electric charge picked up by the film. The effect was apparently the same as reported by Jahn and Weimer (ref. 23). The charge pickup results in spurious signals much larger than those due to the temperature when the bridge circuit is grounded. Even with a floating bridge circuit the spurious signals were the same order of magnitude as the temperature effect. Therefore, the nickel films used at shock speeds above Mach number 4.5 were coated with a thin evaporated layer of silicon monoxide. This effectively reduced the charge pickup, but also increased the response time of the detector. A layer of SiO about 900 Å thick was used over the nickel films in the present case. If the temperature distribution through the silicon is given by

$$T=T_0-(T_0-T_s)\ \mathrm{erf}\frac{x}{\sqrt{4a_st}}$$

then measurements of surface temperature at the depth Δx from the surface will be in error by about $\Delta x/\sqrt{4at}$. If Δx is about 10^{-5} cm and the diffusivity a is about 0.008 cm²/sec for SiO, then the error at 10 microseconds is about 5½ percent. This is considerably less than the variation in the data (fig. 10).

No attempt was made to optimize the silicon monoxide coating procedure. It was found, however, that the nickel films should be baked prior to application of the coating, and that the SiO should be evaporated in a clean environment onto a clean film. Otherwise, erratic and nonlinear calibration of the film resulted. Even the most carefully coated films varied from one another in the value of α by as much as 20 percent, about twice the variation observed in the uncoated films. This variation is accounted for in the calibration, of course, but it may be an indication of some additional instability in the film.

In conclusion, the nickel film surface temperature detectors developed for the present experiments were found suitable for preliminary investigations of the heat flux through gases. However, they are at present the weakest link in the experiments, and most of the variation in the data (fig. 10) is attributable to instabilities in this instrument. Temperature detectors of greater stability and durability, of more uniform calibration, and free from charge accumulation or shunting effects are needed for more precise determination of the thermal conduction properties of high-temperature gases.

REFERENCES

1. Carslaw, H. S., and Jaeger, J. C.: Conduction of Heat in Solids. Oxford, The Clarendon Press, 1947.
2. Jakob, Max: Heat Transfer. Vol. I and II. John Wiley & Sons, 1949, 1957.
3. Kennard, E. H.: Kinetic Theory of Gases. McGraw-Hill Co., 1938.
4. Eggers, A. J., Jr., Hansen, C. Frederick, and Cunningham, Bernard E.: Stagnation-Point Heat Transfer to Blunt Shapes in Hypersonic Flight, Including Effects of Yaw. NACA TN 4229, 1958.
5. Nernst, W.: Chemisches Gleichgewicht und Temperaturgefalle. Ludwig Boltzmann Festschrift, verlag von J. A. Barth, Leipzig, 1904, pp. 904–915.
6. Hirschfelder, Joseph O.: Heat Transfer in Chemically Reacting Mixtures. I. Jour. Chem. Phys., vol. 26, no. 2, Feb. 1957, pp. 274-281.
7. Coffin, Kenneth P., and O'Neal, Cleveland, Jr.: Experimental Thermal Conductivities of the $N_2O_4 \rightleftarrows 2NO_2$ System. NACA TN 4209, 1958.
8. Langmuir, Irving: Convection and Conduction of Heat in Gases. Phys. Rev. vol. 34, no. 6, June 1912, pp. 401–422.
9. Crank, J.: The Mathematics of Diffusion. Oxford, The Clarendon Press, 1956.
10. Boltzmann, L.: Zur Integration der Diffusionsgleichung bei variabeln Diffusionscoefficienten. Annalen der Physik, Leipzig, vol. 53, 1894, pp. 959–964.
11. Butler, James N., and Brokaw, Richard S.: Thermal Conductivity of Gas Mixtures in Chemical Equilibrium. Jour. Chem. Phys., vol. 26, no. 6, June 1957, pp. 1636–1643.
12. Hansen, C. Frederick: Approximations for the Thermodynamic and Transport Properties of High-Temperature Air. NACA TN 4150, 1958.
13. Mersman, W. A., Berggren, W. P., and Boelter, L. M. K.: The Conduction of Heat in Composite Infinite Solids. U. of Calif. Publications in Engineering, vol. 5, no. 1, 1942, pp. 1–22.
14. Smiley, Edward F.: The Measurement of the Thermal Conductivity of Gases at High Temperatures with a Shocktube; Experimental Results in Argon at Temperatures Between 1,000° K and 3,000° K. A Dissertation. Catholic University of America Press, 1957.
15. Glass, I. I., and Patterson, G. N.: A Theoretical and Experimental Study of Shock-Tube Flows, Jour. Aero. Sci., vol. 22, no. 2, Feb. 1955, pp. 73–100.
16. Hansen, C. Frederick, and Heims, Steve P.: A Review of the Thermodynamic, Transport, and Chemical Reaction Rate Properties of High-Temperature Air. NACA TN 4359, 1958.
17. Gilmore, F. R.: Equilibrium Composition and Thermodynamic Properties of Air to 24,000° K. Rand Rep. RM–1543, 1955.
18. Bethe, H. E., and Teller, E.: Deviations from Thermal Equilibrium in Shock Waves. BRL Rep. X–117, Aberdeen Proving Ground, Md., 1945.
19. Blackman, V.: Vibrational Relaxation in Oxygen and Nitrogen. Jour. Fluid Mech., vol. 1, pt. 1, May 1956, pp. 61–85.
20. Camac, M., Camm, J., Keck, J., and Petty, C.: Relaxation Phenomena in Air Between 3,000 and 8,000° K. AVCO Research Lab, Res. Rep. 22, March 13, 1958.
21. Gray, D. E., ed.: American Institute of Physics Handbook. McGraw Hill Book Co., 1957.
22. Rabinowicz, J., Jessey, M. E., and Bartsch, C. A.: Resistance Thermometer for Heat Transfer Measurements in a Shock Tube. GALCIT Memo 33, Calif. Inst. of Tech., July 2, 1956.
23. Jahn, Robert G., and Weimer, David: On the Performance of Thin-Film Gauges in High-Temperature Shock Tube Flows. Jour. Appl. Phys., vol. 29, no. 4, pp. 741–742, April 1958.

U.S. GOVERNMENT PRINTING OFFICE: 1960